Molecular Neurobiology

A REST-dependent presynaptic homeostasis induced by chronic neuronal hyperactivity

--Manuscript Draft--

Manuscript Number:	MOLN-D-17-00109
Article Type:	Original Article
Keywords:	Homeostatic plasticity, REST, gene transcription, excitatory synapse, neuronal excitability, presynaptic terminal, synaptic vesicles
Corresponding Author:	Pietro Baldelli, PhD Universita degli Studi di Genova Genova, Genova ITALY
First Author:	Federico Pecoraro Bisogni, PhD
Order of Authors:	Federico Pecoraro Bisogni, PhD
	Gabriele Lignani, PhD
	Andrea Contestabile, PhD
	Enrico Castroflorio, PhD
	Davide Pozzi, PhD
	Marta Orlando, PhD
	Manuela Massacesi, B.Pharm.
	Pierluigi Valente, PhD
	Fabio Benfenati, MD
	Pietro Baldelli, PhD
Abstract:	Homeostatic plasticity is a regulatory feedback response in which either synaptic strength or intrinsic excitability can be adjusted up or down to offset sustained changes in neuronal activity. Although a growing number of evidences constantly provide new insights into these two apparently distinct homeostatic processes, a unified molecular model remains unknown. We recently demonstrated that REST is a transcriptional repressor critical for the downscaling of intrinsic excitability in cultured hippocampal neurons subjected to prolonged elevation of electrical activity. Here we report that, in the same experimental system, REST also participates in synaptic homeostasis by reducing the strength of excitatory synapses by specifically acting at the presynaptic level. Indeed, chronic hyperactivity triggers a REST-dependent decrease of the size of synaptic vesicle pools through the transcriptional repression of several presynaptic REST-target genes. Together with our previous report, the data identify REST as a fundamental molecular player for neuronal homeostasis able to downscale simultaneously both intrinsic excitability and presynaptic efficiency in response to elevated neuronal activity. This experimental evidence adds new insights to the complex activity-dependent transcriptional regulation of homeostatic plasticity processes.

REST-dependent presynaptic homeostasis induced by chronic neuronal hyperactivity

Abbreviated title: **REST-dependent synaptic scaling-down**

Pecoraro-Bisogni F.[1,2^], Lignani G.[2a^], Contestabile A.[2], Castroflorio E.[2], Pozzi D.[2b], Orlando M.[2c], Valente P[1], Massacesi M.[2d], Benfenati F[1,2] and Baldelli P.[1,2]

[1]Department of Experimental Medicine, Section of Physiology, University of Genova, Viale Benedetto XV, 3, 16132 Genova, Italy;
[2]Center for Synaptic Neuroscience and Technology, Istituto Italiano di Tecnologia, Largo Rosanna Benzi 10, 16132 Genova, Italy

^equal contribution

Present addresses:

[a]Institute of Neurology, University College of London, London WC1N 3BG, UK
[b] *present address:* Pharmacology and Brain Pathology Lab, Humanitas Clinical and Research Center, Humanitas University, Via Manzoni 56, Rozzano, Milan, Italy
[c] *present address:* Neurocure NWFZ, Charite Universitaetsmedizin Berlin, Chariteplatz 1, 10117 Berlin, Germany
[d] *present address:* Laboratory of Neurosciences and Neurogenetics, Department of Head and Neck Diseases, "G. Gaslini" Institute, Via Gerolamo Gaslini 5, 16147 Genova Italy

Corresponding Authors:

Pietro Baldelli, PhD
Department of Experimental Medicine, Section of Physiology, University of Genova, Viale Benedetto XV, 3, 16132 Genova, Italy
pietro.baldelli@unige.it

Gabriele Lignani,PhD
University College of London, London WC1N 3BG, UK
g.lignani@ucl.ac.uk

Abstract

Homeostatic plasticity is a regulatory feedback response in which either synaptic strength or intrinsic excitability can be adjusted up or down to offset sustained changes in neuronal activity. Although a growing number of evidences constantly provide new insights into these two apparently distinct homeostatic processes, a unified molecular model remains unknown. We recently demonstrated that REST is a transcriptional repressor critical for the downscaling of intrinsic excitability in cultured hippocampal neurons subjected to prolonged elevation of electrical activity. Here we report that, in the same experimental system, REST also participates in synaptic homeostasis by reducing the strength of excitatory synapses by specifically acting at the presynaptic level. Indeed, chronic hyperactivity triggers a REST-dependent decrease of the size of synaptic vesicle pools through the transcriptional repression of several presynaptic REST-target genes. Together with our previous report, the data identify REST as a fundamental molecular player for neuronal homeostasis able to downscale simultaneously both intrinsic excitability and presynaptic efficiency in response to elevated neuronal activity. This experimental evidence adds new insights to the complex activity-dependent transcriptional regulation of homeostatic plasticity processes.

Keywords

Homeostatic plasticity, REST, gene transcription, excitatory synapse, neuronal excitability, presynaptic terminal, synaptic vesicles

Introduction

Intrinsic and synaptic homeostases represent the two most relevant mechanisms of homeostatic plasticity in neurons. Although several molecular pathways underlying these two forms of neuronal homeostasis have been identified [1-5], the scenario is becoming every day more puzzling and fragmented, and intrinsic and synaptic homeostases are often seen as two distinct processes. Moreover, the "single candidate gene"-based study of homeostatic plasticity processes h_as started to be substituted by a wider multiple gene modification prospective [6,5]. Indeed, the simultaneous regulation of thousands of genes and proteins to compensate for sustained alterations in network activity has been reported [5,6]. The crucial action of activity-dependent transcription factors regulating the expression of several target-genes in response to change in the level of network activity is a likely possibility and starts to be experimentally addressed. However, the molecular mechanisms governing the activity-dependent reorganization of the transcriptional profile are still to be elucidated.

REST is a zinc-finger transcription factor initially identified as a gene repressor central for neuronal differentiation [7-9]. Many studies, conducted on neural stem cells and neural progenitors [10-14], have led to a unified view in which a progressive downregulation of REST activity during neuronal development de-represses many neuronal genes [15] crucial for processes such as axonal growth, formation of synaptic contacts and membrane excitability that trigger the morphological and functional differentiation of mature neurons [16-20,9]. Besides its physiological role, dysregulation of REST activity was reported in pathological states such as ischemia [21-24] and epileptic seizures [25-27]. For its repressive action on several neuronal genes, REST could be a potential actor in the complex transcriptional re-rearrangement at the basis of the homeostatic processes.

We have recently demonstrated that REST mRNA and protein are up-regulated in cultured hippocampal neurons subjected to chronic hyperactivity. Such increase of REST expression was associated with the down-regulation of voltage-gated sodium channels, Nav1.2 [28], which enabled the recovery of the physiological firing activity, demonstrating, for the first time, an involvement of REST in hyperactivity-induced intrinsic homeostasis. Although sodium channels represent one of the main REST-target genes, many synaptic genes can be regulated by REST [29-31], thus opening the possibility that it might also be involved in synaptic scaling.

Here, using the same model of chronic neuronal hyperactivity in cultured hippocampal neurons previously adopted to characterize the REST effects on intrinsic excitability [28], we identify a parallel action of REST in the regulation of synaptic homeostasis. Indeed, through a complex downregulation of mRNAs coding for multiple presynaptic proteins, REST scales down the efficiency of neurotransmitter release mainly acting on the efficiency of the presynaptic machinery.

Notably, this represents the first experimental evidence of a hyperactivity-induced transcriptional pathway capable of activating both intrinsic and synaptic homeostasis, thus suggesting REST as a transcriptional hub of these two homeostatic processes. This evidence further indicates the existence of a deep molecular intertwinement between different forms of homeostatic plasticity, adding a new layer of complexity in the already puzzling scenario of the signalling pathways underlying homeostatic plasticity.

Materials and Methods

Primary cultures of dissociated hippocampal and cortical neurons

All experiments were performed in accordance with the guidelines established by the European Communities Council (Directive 2010/63/EU of September 22, 2010) and were approved by the Italian Ministry of Health. Pregnant mice C57BL/6J (Charles River) were sacrificed by inhalation of CO_2, and embryonic day 17-18 (E17-18) embryos of either sex were removed immediately by caesarean section. Removal and dissection of cortices and hippocampi, isolation of neurons and culturing procedures were as those previously described [32]. Briefly, skulls were opened and brains were dissected out and placed into Hank's Balanced Salt Solution (HBSS). Hippocampi and cortices were removed under a dissecting microscope and collected. After 15 min of incubation with 0.25% trypsin in HBSS at 37 °C, whole hippocampi and cortices were washed with HBSS to remove trypsin and then mechanically dissociated. Neurons stained with a vital dye (Trypan blue; Sigma-Aldrich) were counted by using a Burker chamber. Neurons were plated on poly-L-lysine (0.1 mg/ ml; Sigma- Aldrich)-treated 25 mm glass coverslips or Petri dishes at a density of 80,000 cells per coverslip (low-density cultures). Cells were plated and maintained in culture medium consisting of Neurobasal, B-27 (1:50 v/v), glutamax (1% w/v), and penicillin-streptomycin (1%) at 37 °C in a 5% CO_2 humidified atmosphere. All experiments were performed on mature neurons older than 16 days *in vitro* (div). At this stage, hippocampal cultures contained approximately ~80% excitatory glutamatergic neurons and approximately ~20% GABAergic inhibitory interneurons [33].

To induce neuronal hyperactivity, we used the non-selective potassium channel blocker 4-aminopirydine (4AP), a widely adopted model of *epileptogenesis* in brain slices ([34] for review) that was also recently used in cultured neurons to induce network hyperactivity [28,35]. 4AP (100 µM) was dissolved in complete Neurobasal medium, applied to neuronal

cultures and maintained for the indicated times. The treatment was stopped after 24 hr for RT-qPCR analysis and after 48 hr for patch-clamp, electron microscopy or fluorescence imaging analyses. The different time intervals are due to the previously shown physiological delay necessary for an initial transcriptional change to be translated into protein expression and functional effects[28].

RNA interference, lentivirus production and infection procedures

The REST/NRSF target sequence used to generate shRNA 1032 (5'-ACATGCAAGACAGGTTCACAA-3') was previously identified and validated [28]. The shRNA construct was obtained by cloning this sequence into pcDNA6.2-GW/EmGFP-miR plasmid using a microRNA (miR)-based expression vector kit (BLOCK-iT Pol II miR; Invitrogen) according to the manufacturer's instructions, thereby creating an expression cassette consisting of the 5' miR flanking region, the REST-target sequence and the 3' miR flanking region. As a negative control, the pcDNA6.2-GW/EmGFP-miR-neg plasmid (Invitrogen) containing a sequence not targeting any known vertebrate gene was used. These cassettes, expressing either control shRNA or against REST were then sub-cloned into the lentiviral (LV) vector pCCL.sin.cPPT.PGK.GFP.WPRE (a kind gift from M. Amendola and L. Naldini, TIGET, San Raffaele Sci. Institute, Milan, Italy) or in the same vector in which GFP was substituted with mCherry fluorescent protein. Third-generation LVs were produced by transient four-plasmid co-transfection into HEK293T cells using the calcium phosphate transfection method. Supernatants were collected, passed through a 0.45 μm filter and purified by ultracentrifugation as previously described. Viral vectors were titrated at concentrations ranging from 1 x 10^8 to 5 x 10^9 transducing units (TU)/ml. Cultures were infected at 10 div by using 10 multiplicity of infection (MOI), and neurons were checked for infection at 14 div. The efficiency of infection was estimated to range

between 80 and 95% by counting neurons expressing GFP protein with respect to the total number of cells stained with DAPI.

Real-time PCR (RT-qPCR)

RNA was extracted with TriaZol reagent and purified on RNeasy spin columns (Qiagen). RNA samples were quantified at 260 nm with an ND1000 Nanodrop spectrophotometer (Thermo Scientific). Reverse transcription was performed according to the manufacturer's recommendations on 1 µg of RNA with the QuantiTect Reverse Transcription Kit (Qiagen), which includes a genomic DNA–removal step. SYBR green RT-qPCR was performed in triplicate with 10 ng of template cDNA using QuantiTect Master Mix (Qiagen) on a 7900-HT Fast Real-time System (Applied Biosystems) as previously described [28,36] and using the following universal conditions: 5 min at 95 °C, 40 cycles of denaturation at 95 °C for 15 s, and annealing/extension at 60 °C for 30 s. Product specificity and occurrence of primer dimers were verified by melting-curve analysis. Primers were designed with Beacon Designer software (Premier Biosoft) to avoid template secondary structure and significant cross homology with other genes by BLAST search. The PCR reaction efficiency for each primer pair was calculated via the standard curve method with four serial-dilution points of cDNA. The PCR efficiency calculated for each primer set was used for subsequent analysis. All experimental samples were detected within the linear range of the assay. Gene-expression data were normalized via the multiple-internal-control-gene method[37] with the GeNorm algorithm available in qBasePlus software (Biogazelle). The control genes used were GAPDH (glyceraldehyde-3-phosphate dehydrogenase) and PPIA (peptidylprolyl isomerase). The expression of these genes was found not to be affected by the 4AP treatment.

GAPDH-F: GAACATCATCCCTGCATCCA; GAPDH-R: CCAGTGAGCTTCCCGTTCA;

PPIA-F: CACTGTCGCTTTTCGCCGCTTG; PPIA-R:

TTTCTGCTGTCTTTGGAACTTTGTCTGC; REST-F: GAACCACCTCCCAGTATG; REST-R: CTTCTGACAATCCTCCATAG; mAMPA1-F : GGCATGGCATGTGAAGCAATG; mAMPA1-R : GGAGTCTACAGTAGTAGGCAGGAGSNAP25-F: CCTAGTAGGTCTTGCACATACAC; SNAP25-R: GACAGAGCACACAGGACATTT; Synaptotagmin2 (Syt2)-F: GGCGGCGAGATGTGATAC; Syt2-R: AAGCCATGACTGACAAGAGG; Synaptophysin (SYPH)-F: TTCAGTGCTTGGAATCTAC; SYPH-R: TTCTCCAGAGTGAAGTCG; VGlUT1-F: TTACAGAATCCCAGGAAAGG; VGLUT1-R: TCACAGAGACAGACACCA; Synapsin1 (Syn1)-F: ATCTTCCTCCAACCTCCA; Syn1-R: TTTGCTTCCCGACTCTTC.

Immunocytochemistry

Primary hippocampal neurons infected at 10 div with lentiviral vectors expressing scrambled or shRNA were treated at 16 div and fixed at 18 div with 4% paraformaldehyde in 0.1 M phosphate buffer, pH 7.4, for 20 min at room temperature.

After several washes in PBS, they were permeabilized and blocked for 30 min in 5% normal goat serum (NGS), 0.1% saponin in PBS and then incubated with primary antibodies: mouse anti-β3Tubuline (1:500,Covance) and guinea pig anti-VGLUT-1 (1:1000,Synaptic System) diluted in 5% NGS and 0.1% saponin in PBS up to 2 h.

Coverslips were then washed twice in 0.1% saponin in PBS and blocked for 10 min in 5% NGS and 0.1% saponin in PBS before being incubated in the same buffer with AlexaFluor-conjugated secondary antibodies (1:500; Invitrogen). After several washes in PBS, coverslips were mounted using Prolong Gold antifade reagent containing DAPI staining (Invitrogen). Primary antibodies were omitted to control for the specificity of the staining. Images were acquired using a 60x oil objective in a Leica SP5 confocal. Acquired images were analyzed using ImageJ software.

The intensity of each excitatory terminal has been calculated as average intensity of the region of interest (ROI) that circumscribes the VGLUT1 positive synaptic signal. The VGLUT1 synaptic densities on dendrites were obtained by counting the total number of positive puncta divided by the length of the tubulin positive segment (in µm). The number of samples (n) represents the number of coverslips from at least 3 neuronal preparations conducted in parallel. From each coverslip, at least 10 –15 images were collected.

Patch-clamp recordings from dissociated cultured hippocampal neurons

Whole-cell patch-clamp recordings of AMPA-mediated miniature EPSCs (mEPSCs) were obtained in presence of tetrodotoxin (TTX, 1 µM), as previously described [38]. Patch pipettes, prepared from thin borosilicate glass (Hilgenberg), were pulled and fire-polished to a final resistance of 4–5 MΩ when filled with standard internal solution. Neurons were infected at 10 div, treated with 4AP at 16 div and recorded at 18 div. mEPSCs were recorded from cultured pyramidal neurons, morphologically identified by their teardrop-shaped somata and characteristic apical dendrite, using a double EPC-10 amplifier (HEKA Electronic, Lambrecht, Germany). Cells were maintained in a standard external solution (Tyrode) containing (in mM): 140 NaCl, 2 $CaCl_2$, 1 $MgCl_2$, 4 KCl, 10 glucose, and 10 HEPES (pH 7.3 with NaOH). Unless otherwise indicated, δ-(-)-2-amino-5-phosphonopentanoic acid (D-APV; 50 µM; Tocris), bicuculline methiodide (30 µM, Tocris) and ((2S)-3-[[(1S)-1-(3,4-Dichlorophenyl) ethyl]amino-2hydroxypropyl] (phenylmethyl) phosphinic acid hydrochloride; CGP58845 hydrochloride; 5 µM) and TTX (300 nM), were added to the Tyrode external solution to block N-methyl-δ- aspartate (NMDA) $GABA_A$Rs, $GABA_B$Rs and voltage gated Na^+ channels, respectively. The standard internal solution contained (in mM): 126 K^+ Gluconate, 4 NaCl, 1 $MgSO_4$, 0.02 $CaCl_2$, 0.1 BAPTA, 15 glucose, 5 HEPES, 3 ATP, and 0.1 GTP (pH 7.2 with KOH). Experiments were performed

at 22–24 °C and Miniature EPSCs were acquired at 20 kHz sample frequency and filtered at half the acquisition rate with an 8-pole low-pass Bessel filter.

Recordings with leak currents >100 pA or series resistance >20 MΩ were discarded. Data acquisition was performed using PatchMaster program (HEKA Elektronic). The mEPSCs analysis was performed by using the Minianalysis program (Synaptosoft, Leonia, NJ and the Prism software (GraphPad Software, Inc.). The amplitude and frequency of mEPSCs were calculated using a peak detector function with a threshold amplitude set at 4 pA and a threshold area at 50 ms*pA.

Electron Microscopy

Neurons were infected at 10 div, treated for 48 hours with 4AP at 16 div and fixed at 18 div with 1.2% glutaraldehyde in 66 mm sodium cacodylate buffer, post fixed in 1% OsO_4, 1.5% $K_4Fe(CN)_6$, 0.1 m sodium cacodylate, en bloc stained with 1% uranyl acetate, dehydrated, and flat embedded in epoxy resin (Epon 812, TAAB). After embedding, the glass coverslip was removed from the Epon block by thermal shock and neurons were identified under a stereomicroscope. Embedded neurons were then excised from the block and mounted on a cured Epon block for sectioning, using an EM UC6 ultra-microtome (Leica Microsystem). Ultrathin sections (60–70 nm thick) were collected on 200-mesh copper grids (EMS) and observed with a JEM-1011 electron microscope (Jeol, Tokyo, Japan) operating at 100 kV using an ORIUS SC1000 CCD camera (Gatan, Pleasanton, CA). For each experimental condition 30 images were acquired at 10,000x magnifications (sampled area per experimental conditions: 136.5 μm^2). Synaptic profile area, SV number and the other morphometric data were determined using ImageJ software.

Fluorescent live-cell imaging

Primary hippocampal neurons were maintained in Tyrode's solution supplemented with CNQX 10 μM; APV 50 μM) through a laminar flow perfusion system. The lentiviral vector expressing Synaptophysin–pHluorin (SypHy) was prepared as previously described [39]. Viral titers ranging from 1.0 to 5.0 × 10^8 transforming units/ml were obtained. Primary hippocampal neurons were infected with SypHy and either shRNA/scramble-mCherry at 10 div at 10 multiplicity of infection. After 24 h, half of the medium was replaced with fresh medium. All experiments were performed between 16 and 18 DIV. Images were captured at 1Hz and at a depth of 16-bits using a QuantEM 512 SC camera (Photometrics) and a UplanSapo 60X1.35 NA oil-immersion objective (Olympus). For electrical field stimulation, coverslips were mounted into the imaging chamber (~100 ul volume; Quick Exchange Platform; Warner Instruments) and action potentials (APs) were evoked by passing 1 ms biphasic current pulses through platinum iridium electrodes using an AM2100 stimulator (AM-Systems).

To evaluate the effects of 4AP on SV pool sizes, stimulation protocols were applied to estimate the release from either the readily releasable pool (40 action potentials at 20 Hz) or the recycling pool (900 action potentials at 20 Hz) in the presence of bafilomycin, as previously described [40]. The typical experiment was performed as following: after 10 s of baseline acquisition (F_0), neurons were stimulated with a train of 40 stimuli at 20 Hz, then with a longer train of 900 APs at 20Hz in the presence of 1 μM bafilomycin. At the end of the stimulation protocol, cells were perfused with 50 mM NH_4Cl (F_{max}). Images were analyzed using the Simple PCI (Hamamatsu) and custom-written software scripts.

One image was acquired in the red channel at the beginning of each experiment to verify the relative expression of shRNA or scramble on the nucleus. Then, the video acquired in the green channel at a frame rate of 1 Hz was analyzed using the Simple PCI and custom-written software scripts to monitor pH-sensitive change of fluorescence of SypHy-GFP.

Circular ROIs of 1.7 μm diameter were positioned manually at the center of each responsive synapse. Quantitative measurements of fluorescence intensity at individual boutons were obtained by averaging pixel intensity within each ROI. Images were acquired with constant gain and exposure times across all experiments. The total increase in the fluorescence signal (ΔF) was calculated by subtracting F_0 and the ΔF was normalized to the fluorescence value obtained by alkalization of the entire SV pool using NH_4Cl (ΔF_{max}). Data are expressed as means ± SEM for the number of coverslips analyzed. The number of synapses analyzed per coverslip ranged between 20 and 40. Three to five cell preparations were performed for each experimental condition.

Statistical analysis

The statistical analysis is presented in the figure legends. Data are given as means ± SEM for n = sample size. The normal distribution of experimental data was assessed using D'Agostino-Pearson's normality test. The F-test was used to compare variance between two sample groups. To compare two normally distributed sample groups, the Student's paired/unpaired two-tailed *t*-test was used, with Welch's correction applied when variance of the two groups was different. To compare two groups that were not normally distributed, we used Mann–Whitney's non-parametric U-test. To compare more than two groups (scr, scr-4AP, sh, sh-4AP) we used two-way ANOVA, followed by Sidak's post hoc test for functional analysis. The test was used to answer the following questions: (a) did 4AP treatment have effect on various functional and molecular parameters in scramble and shRNA infected neurons? (b) did silencing of REST by shRNA infection affect the results? c) did the duration of the 4AP treatment (24 *vs* 48 h) differently affect the results? Alpha levels for all tests were 0.5% (95% confidence intervals). Statistical analysis was carried out using the Prism software (GraphPad Software, Inc.).

Results

REST-induction by neuronal hyperactivity reduces the frequency of mEPSCs and the intensity of VGLUT1 positive puncta

Application of 4AP was effective in boosting the rate of the spontaneous activity present in functionally mature (>13-15 div) cultured neuronal networks, while it was ineffective in immature neurons where spontaneous activity is still lacking (<10-12div). We previously reported [28] that REST mRNA undergoes a fast and transient upregulation that peak at 24 hrs, followed by a delayed increase of REST protein that becomes significantly apparent after 48 hrs.

Here, we investigated whether such hyperactivity-dependent REST increase exerts a role in the homeostasis of hippocampal excitatory synapses.

To evaluate the effect of chronic heightened activity on excitatory synaptic strength, avoiding the interference of the previously reported REST effect on intrinsic excitability [28], miniature Excitatory Postsynaptic Currents (mEPSCs) were recorded in presence of TTX (1 μM). While the amplitude of mEPSCs reflects the postsynaptic effects of the neurotransmitter and its quantal content in single SVs, mEPSCs frequency is dependent on the number of active synapses and on the stochastic fusion properties of single SVs [41].

This experiment was set as followed: i) non-infected neurons treated for 48 h (from 16 to 18 div) with either vehicle or 4AP (ctrl; 4AP); ii) untreated and 4AP-treated infected neurons at 10 div with lentiviral vectors expressing either the REST-silencing shRNA (sh; sh-4AP) [28] or its scramble sequence (scr; scr-4AP). The same experimental scheme (Fig. 1A) was adopted for all the experiments.

We found that sustained (48 h) neuronal hyperactivity decreased the frequency and amplitude of mEPSCs in both non-infected (Fig. 1B,C) and scr-infected neurons as analyzed at 18 div (Fig. 1B,D). Interestingly, REST knockdown fully prevented the reduction of mESPCs frequency evoked by 4AP treatment, whilst the 4AP-mediated effect on amplitude remained unaffected (Fig. 1D, *left and right panel*). As it is well accepted that the amplitude of mEPSCs reflects postsynaptic effects, whereas mEPSCs frequency is dependent on presynaptic properties [41], our data would suggest a specific role of REST at the presynaptic level.

Such REST-dependent effect could therefore be ascribed to changes at presynaptic terminals, in terms of the number of active synapses and/or to a modulation of the presynaptic release machinery. It was previously demonstrated that prolonged hyper-excitation, induced by $GABA_A$ receptor blockade, downregulates VGLUT1 intensity in putative cortical excitatory synapses [42], and that variations in VGLUT1 expression critically affect the efficacy of glutamatergic synaptic transmission [43]. These evidences prompted us to perform immunocytochemical analysis of VGLUT1-positive puncta in our model of 4AP-induced neuronal hyperactivity (Fig. 2A). We found a significant decrease in the mean fluorescence intensity of VGLUT1 puncta in 4AP-treated non-infected or scr-infected neurons neurons (Fig. 2B,C, *left*). Interestingly, REST knockdown in shRNA-infected neurons virtually suppressed the reduction of VGLUT1 fluorescence intensity induced by neuronal hyperactivity (Fig. 2C, *left*). The density of VGLUT1 positive puncta was not affected by 4AP in both non-infected neurons (Fig. 2B, *right*), as well as in scr-infected neurons (Fig. 2C, *right*). However, in shRNA-infected neurons, 4AP increased the density of VGLUT1 positive puncta (Fig. 2C, *right*), revealing a REST-dependent

homeostatic control also on the density of VGLUT1 positive puncta that is lost when REST is knocked-down.

REST-dependent control on the size of the synaptic vesicle pools

The decreased intensity of VGLUT1 within single synaptic puncta suggested a possible effect on the size of synaptic vesicle (SV) pools [44]. Thus, we performed a functional analysis of single synaptic contacts by using the Synaptophysin-pHluorin (SyPhy) reporter of SV fusion to monitor changes in SV trafficking and size of distinct SV pools [39] upon chronic hyperactivity. By applying appropriate field stimulation protocols to mobilize the various SV pools (Fig. 3A), we found that chronic hyperactivity significantly decreased the size of both the readily releasable pool (RRP; Fig. 3 B,C) and the recycling pool (RP; Fig. 3D,E) in scr-infected neurons. Strikingly, the infection of neurons with REST shRNA completely reverted such effects, so that both RRP and RP sizes were significantly increased in chronic 4AP-treated neurons in which REST was silenced (Fig. 3C,E). These results demonstrate that REST plays a fundamental role in the homeostatic control of functional SV pool size upon high neuronal activity.

These experiments were also paralleled by ultrastructural analysis of excitatory synapses (Fig. 4A) to assess the density and localization of SVs within single terminals. Electron microscopy analysis revealed that 4AP treatment did not affect the overall SV density (Fig. 4B, *upper panel*), but markedly reduced the density of docked SVs, an effect that was totally abolished by REST silencing (Fig. 4B, *lower panel*). The functional results obtained with SypHy (Fig. 3B-E), showing a reduction of RRP and RP sizes, are coherent with the reduced density of docked vesicles (Fig. 4B), even if the two results cannot be directly correlated. However, these data, together with the decrease of mEPSC frequency and VGLUT1 intensity, strongly suggest that REST dynamically regulates SV pools in an

activity-dependent manner, probably through a transcriptional regulation of synaptic REST-target genes involved in SV trafficking as well as in the structural assembly of SV pools.

REST-dependent presynaptic homeostasis is based on the transcriptional regulation of key presynaptic REST target genes

In order to obtain further insights into this REST-dependent transcriptional regulation, we investigated the 4AP-mediated changes in presynaptic genes, relevant for the function of the presynaptic release machinery. As previously observed [28], RT-qPCR analysis showed that a treatment with 4AP for 24h transiently increased REST mRNA levels in scr-infected neurons, while expression of REST shRNA fully prevents this increase (Fig. 5A, *upper panel*).

Although the spontaneous fusion machinery is quite complex and involves several proteins, AMPA receptors are the main determinants of mEPSC amplitude recorded in presence of NMDA blockers. Accordingly, chronic treatment with 4AP persistently decreased AMPA mRNA at both 24 and 48h (Fig. 5A, *center panel*). Such effect was observed in both scr- and shRNA-infected neurons, ruling out a direct relationship of this process with REST upregulation (Fig. 5A, *upper panel*) and confirming the REST-independence of the scaling down of the mEPSC amplitude (Fig. 1D)

On the contrary, RT-qPCR analysis showed a transient 4AP-dependent decrease of VGLUT1 mRNA expression that was fully abolished by REST knockdown (Fig. 5A, *lower panel*). Moreover, the mRNA levels of SNAP25, Synapsin1 and synaptotagmin2 involved in controlling the size of the recycling pool of SVs [45] and the efficacy of SVs release [46] were strongly downregulated upon 4AP treatment in a REST-dependent manner (Fig. 5 B).

These data strongly support a role of REST in the homeostatic control of presynaptic properties.

Discussion

Here, we reported that chronic neuronal hyperactivity induces two distinct forms of synaptic homeostasis affecting glutamatergic synaptic transmission: a REST-independent postsynaptic effect and a REST-dependent presynaptic modulation. The latter process consists in a novel form of REST-dependent homeostasis occurring selectively at presynaptic terminals, characterized by a decrease in mEPSC frequency associated with a reduced intensity of VGLUT1-positive contacts and VGLUT-1 mRNA levels. Moreover, we also observed that REST-mediated presynaptic homeostasis also decreases the readily releasable pool and the recycling pool sizes, the density of docked SVs and the mRNA levels of three fundamental molecular actors of the presynaptic machinery. Previous works reported a down-regulation of VGLUT1/synaptophysin ratio at excitatory synapses after 48 h exposure to bicuculline [42]. Others described a decrease in calcium entry into nerve terminals in response to the action potential associated with a reduction in the probability of SV fusion in cultured hippocampal neuron treated with gabazine for 48h [47]. Despite these compelling evidences of presynaptic homeostasis, no clear mechanistic explanations were proposed.

Our results provide a molecular explanation for the previously observed processes of presynaptic homeostasis triggered by sustained hyperactivity [41,46]. We demonstrate the existence of a REST-dependent transcriptional rearrangement able to scale down the strength of excitatory synapses by modulating the transcriptional profile of multiple REST-target genes involved in the structural and functional regulation of the presynaptic release machinery.

Together with our previous findings of a REST involvement in the negative control of neuronal firing upon elevated neuronal activity, the present data suggest the existence of a molecular interplay between intrinsic homeostatic plasticity and synaptic scaling, in which

REST might be the common molecular player. While it is widely accepted that a chronic perturbation of neuronal network activity triggers these two forms of homeostatic plasticity, they are considered to a large extent independent. Here, we provide evidences that homeostatic plasticity phenomenon should not be conceived as a series of distinct molecular events occurring at different neuronal sites, but rather as a unified process in which synaptic scaling and intrinsic excitability can be simultaneously modulated by a common molecular players, like REST.

The limitations of our study are mainly associated with the lack of a full picture, representing the entire transcriptional homeostatic changes induced by network hyperactivity. Indeed, we focused our analysis on a limited number of mRNAs coding for those presynaptic proteins potentially involved in the REST-dependent functional rearrangement that we identified. It is likely that many others REST target genes involved in this process and have to be identified. Indeed, recent findings showed the implication of hundreds of proteins in the mechanisms of homeostatic compensation, due to both synaptic scaling-up and scaling-down [5]. These results indicate that homeostatic plasticity can be transcriptionally governed by master regulators, such as REST, that can simultaneously regulate entire families of target-genes and related proteins [5]. A complete mapping of these changes need to be better investigated through transcriptomic and proteomic approaches.

Our findings also contribute to the debate on whether the role of REST upregulation in adult neurons is deleterious or beneficial [48-50,29,51]. It has been shown that REST upregulation upon ischemic insults leads to neuronal death, while its acute knockdown in hippocampal slices subjected to oxygen/glucose deprivation prevents neuronal damage [21-23,52,24]. Moreover, in kainate-induced temporal lobe epilepsy REST upregulation aggravates neuronal hyperexcitability through repression of HCN1 channels [31,27]. Despite such evidences, a protective role of REST upregulation was highlighted by other

studies. Indeed, it was shown that the anti-epileptic effect of the ketogenic diet is attributable, at least in part, to the repression of BDNF by REST due to a chromatin remodeling process [53]. According to this initial observation, the conditional deletion of REST in the forebrain excitatory neurons in a kindling model of epileptogenesis accelerated seizure progression and was associated with a significant increase of BDNF following kainic acid-induced *status epilepticus* [54].

A further evidence for a protective role of REST was recently reported. High REST levels were present in normal ageing brain and were associated with the down-regulation of potentially toxic genes involved in oxidative stress and amyloid β-protein toxicity, while low REST levels were present in Alzheimer's brains [55]. In addition, a missense mutation in the REST gene was recently associated with reduced hippocampal volume, suggesting that REST expression may be neuroprotective [56,57].

Altogether, these reports highlight the complex Janus-faced nature of REST signaling: on one hand it exerts an homeostatic and neuroprotective action that may predominate under physiological conditions, on the other it can become detrimental in pathological conditions when neuronal homeostasis is fully lost, thus worsening the progression of the disease.

The results presented here, together with our previous report [28], strengthen the idea of a protective role of REST against perturbations of the normal physiology of neuronal networks and uncover a coordinated homeostatic response based on a REST-dependent functional rescaling of both intrinsic excitability and synaptic properties of neuronal circuits.

Acknowledgements: this study was supported by research grants from Italian Ministry of Health Bando Giovani Ricercatori (GR-2009-1473821 to P.B.); EUFP7 Integrating Project "Desire" (Grant no.602531) and EU ITN ''ECMED'' (Grant no. 642881) to F.B. The support of Telethon-Italy (Grant GGP13033; to F.B.) and CARIPLO Foundation (Grants no. 2013-0879 and 2013-0735 to F.B.) are also acknowledged. We wish to thank Prof. Jacopo

Meldolesi for helpful discussions and Dr. Silvia Casagrande for precious help with cell cultures

Conflict of Interest: the authors declare no competing financial interests.

References

1. Davis GW (2013) Homeostatic signaling and the stabilization of neural function. Neuron 80 (3):718-728. doi:10.1016/j.neuron.2013.09.044

2. Nelson SB, Turrigiano GG (2008) Strength through diversity. Neuron 60 (3):477-482. doi:10.1016/j.neuron.2008.10.020

3. Davis GW (2006) Homeostatic control of neural activity: from phenomenology to molecular design. Annu Rev Neurosci 29:307-323. doi:10.1146/annurev.neuro.28.061604.135751

4. Davis GW, Muller M (2015) Homeostatic control of presynaptic neurotransmitter release. Annu Rev Physiol 77:251-270. doi:10.1146/annurev-physiol-021014-071740

5. Schanzenbacher CT, Sambandan S, Langer JD, Schuman EM (2016) Nascent Proteome Remodeling following Homeostatic Scaling at Hippocampal Synapses. Neuron 92 (2):358-371. doi:10.1016/j.neuron.2016.09.058

6. Meadows JP, Guzman-Karlsson MC, Phillips S, Holleman C, Posey JL, Day JJ, Hablitz JJ, Sweatt JD (2015) DNA methylation regulates neuronal glutamatergic synaptic scaling. Sci Signal 8 (382):ra61. doi:10.1126/scisignal.aab0715

7. Chong JA, Tapia-Ramirez J, Kim S, Toledo-Aral JJ, Zheng Y, Boutros MC, Altshuller YM, Frohman MA, Kraner SD, Mandel G (1995) REST: a mammalian silencer protein that restricts sodium channel gene expression to neurons. Cell 80 (6):949-957

8. Schoenherr CJ, Anderson DJ (1995) The neuron-restrictive silencer factor (NRSF): a coordinate repressor of multiple neuron-specific genes. Science 267 (5202):1360-1363

9. Mandel G, Fiondella CG, Covey MV, Lu DD, Loturco JJ, Ballas N (2011) Repressor element 1 silencing transcription factor (REST) controls radial migration and temporal neuronal specification during neocortical development. Proc Natl Acad Sci U S A 108 (40):16789-16794. doi:10.1073/pnas.1113486108

10. Sun YM, Greenway DJ, Johnson R, Street M, Belyaev ND, Deuchars J, Bee T, Wilde S, Buckley NJ (2005) Distinct profiles of REST interactions with its target genes at different stages of neuronal development. Mol Biol Cell 16 (12):5630-5638. doi:10.1091/mbc.E05-07-0687

11. Greenway DJ, Street M, Jeffries A, Buckley NJ (2007) RE1 Silencing transcription factor maintains a repressive chromatin environment in embryonic hippocampal neural stem cells. Stem Cells 25 (2):354-363. doi:10.1634/stemcells.2006-0207

12. Johnson R, Teh CH, Kunarso G, Wong KY, Srinivasan G, Cooper ML, Volta M, Chan SS, Lipovich L, Pollard SM, Karuturi RK, Wei CL, Buckley NJ, Stanton LW (2008) REST regulates distinct transcriptional networks in embryonic and neural stem cells. PLoS Biol 6 (10):e256. doi:10.1371/journal.pbio.0060256

13. Conaco C, Otto S, Han JJ, Mandel G (2006) Reciprocal actions of REST and a microRNA promote neuronal identity. Proc Natl Acad Sci U S A 103 (7):2422-2427. doi:10.1073/pnas.0511041103

14. Otto SJ, McCorkle SR, Hover J, Conaco C, Han JJ, Impey S, Yochum GS, Dunn JJ, Goodman RH, Mandel G (2007) A new binding motif for the transcriptional repressor REST uncovers large gene networks devoted to neuronal functions. J Neurosci 27 (25):6729-6739. doi:10.1523/JNEUROSCI.0091-07.2007

15. Tapia-Ramirez J, Eggen BJ, Peral-Rubio MJ, Toledo-Aral JJ, Mandel G (1997) A single zinc finger motif in the silencing factor REST represses the neural-specific type II sodium channel promoter. Proc Natl Acad Sci U S A 94 (4):1177-1182

16. Su X, Gopalakrishnan V, Stearns D, Aldape K, Lang FF, Fuller G, Snyder E, Eberhart CG, Majumder S (2006) Abnormal expression of REST/NRSF and Myc in neural stem/progenitor cells causes cerebellar tumors by blocking neuronal differentiation. Mol Cell Biol 26 (5):1666-1678. doi:10.1128/MCB.26.5.1666-1678.2006

17. Paquette AJ, Perez SE, Anderson DJ (2000) Constitutive expression of the neuron-restrictive silencer factor (NRSF)/REST in differentiating neurons disrupts neuronal gene expression and causes axon pathfinding errors in vivo. Proc Natl Acad Sci U S A 97 (22):12318-12323. doi:10.1073/pnas.97.22.12318

18. Aoki H, Hara A, Era T, Kunisada T, Yamada Y (2012) Genetic ablation of Rest leads to in vitro-specific derepression of neuronal genes during neurogenesis. Development 139 (4):667-677. doi:10.1242/dev.072272

19. Nechiporuk T, McGann J, Mullendorff K, Hsieh J, Wurst W, Floss T, Mandel G (2016) The REST remodeling complex protects genomic integrity during embryonic neurogenesis. Elife 5:e09584. doi:10.7554/eLife.09584

20. Cargnin F, Nechiporuk T, Mullendorff K, Stumpo DJ, Blackshear PJ, Ballas N, Mandel G (2014) An RNA binding protein promotes axonal integrity in peripheral neurons by destabilizing REST. J Neurosci 34 (50):16650-16661. doi:10.1523/JNEUROSCI.1650-14.2014

21. Calderone A, Jover T, Noh KM, Tanaka H, Yokota H, Lin Y, Grooms SY, Regis R, Bennett MV, Zukin RS (2003) Ischemic insults derepress the gene silencer REST in neurons destined to die. J Neurosci 23 (6):2112-2121

22. Formisano L, Noh KM, Miyawaki T, Mashiko T, Bennett MV, Zukin RS (2007) Ischemic insults promote epigenetic reprogramming of mu opioid receptor expression in hippocampal neurons. Proc Natl Acad Sci U S A 104 (10):4170-4175. doi:10.1073/pnas.0611704104

23. Noh KM, Hwang JY, Follenzi A, Athanasiadou R, Miyawaki T, Greally JM, Bennett MV, Zukin RS (2012) Repressor element-1 silencing transcription factor (REST)-dependent epigenetic remodeling is critical to ischemia-induced neuronal death. Proc Natl Acad Sci U S A 109 (16):E962-971. doi:10.1073/pnas.1121568109

24. Kaneko N, Hwang JY, Gertner M, Pontarelli F, Zukin RS (2014) Casein kinase 1 suppresses activation of REST in insulted hippocampal neurons and halts ischemia-induced neuronal death. J Neurosci 34 (17):6030-6039. doi:10.1523/JNEUROSCI.4045-13.2014

25. Palm K, Belluardo N, Metsis M, Timmusk T (1998) Neuronal expression of zinc finger transcription factor REST/NRSF/XBR gene. J Neurosci 18 (4):1280-1296

26. Spencer EM, Chandler KE, Haddley K, Howard MR, Hughes D, Belyaev ND, Coulson JM, Stewart JP, Buckley NJ, Kipar A, Walker MC, Quinn JP (2006) Regulation and role of REST and REST4 variants in modulation of gene expression in in vivo and in vitro in epilepsy models. Neurobiol Dis 24 (1):41-52. doi:10.1016/j.nbd.2006.04.020

27. McClelland S, Flynn C, Dube C, Richichi C, Zha Q, Ghestem A, Esclapez M, Bernard C, Baram TZ (2011) Neuron-restrictive silencer factor-mediated hyperpolarization-activated cyclic nucleotide gated channelopathy in experimental temporal lobe epilepsy. Ann Neurol 70 (3):454-464. doi:10.1002/ana.22479

28. Pozzi D, Lignani G, Ferrea E, Contestabile A, Paonessa F, D'Alessandro R, Lippiello P, Boido D, Fassio A, Meldolesi J, Valtorta F, Benfenati F, Baldelli P (2013) REST/NRSF-mediated intrinsic homeostasis protects neuronal networks from hyperexcitability. EMBO J 32 (22):2994-3007. doi:10.1038/emboj.2013.231

29. Baldelli P, Meldolesi J (2015) The Transcription Repressor REST in Adult Neurons: Physiology, Pathology, and Diseases(1,2,3). eNeuro 2 (4). doi:10.1523/ENEURO.0010-15.2015

30. Schoenherr CJ, Paquette AJ, Anderson DJ (1996) Identification of potential target genes for the neuron-restrictive silencer factor. Proc Natl Acad Sci U S A 93 (18):9881-9886

31. McClelland S, Brennan GP, Dube C, Rajpara S, Iyer S, Richichi C, Bernard C, Baram TZ (2014) The transcription factor NRSF contributes to epileptogenesis by selective repression of a subset of target genes. Elife 3:e01267. doi:10.7554/eLife.01267

32. Baldelli P, Fassio A, Valtorta F, Benfenati F (2007) Lack of synapsin I reduces the readily releasable pool of synaptic vesicles at central inhibitory synapses. J Neurosci 27 (49):13520-13531. doi:10.1523/JNEUROSCI.3151-07.2007

33. Ivenshitz M, Segal M (2010) Neuronal density determines network connectivity and spontaneous activity in cultured hippocampus. J Neurophysiol 104 (2):1052-1060. doi:10.1152/jn.00914.2009

34. Avoli M, D'Antuono M, Louvel J, Kohling R, Biagini G, Pumain R, D'Arcangelo G, Tancredi V (2002) Network and pharmacological mechanisms leading to epileptiform synchronization in the limbic system in vitro. Prog Neurobiol 68 (3):167-207

35. Ryan D, Drysdale AJ, Lafourcade C, Pertwee RG, Platt B (2009) Cannabidiol targets mitochondria to regulate intracellular Ca2+ levels. J Neurosci 29 (7):2053-2063. doi:10.1523/JNEUROSCI.4212-08.2009

36. Deidda G, Parrini M, Naskar S, Bozarth IF, Contestabile A, Cancedda L (2015) Reversing excitatory GABAAR signaling restores synaptic plasticity and memory in a mouse model of Down syndrome. Nat Med 21 (4):318-326. doi:10.1038/nm.3827

37. Vandesompele J, De Preter K, Pattyn F, Poppe B, Van Roy N, De Paepe A, Speleman F (2002) Accurate normalization of real-time quantitative RT-PCR data by geometric averaging of multiple internal control genes. Genome Biol 3 (7):RESEARCH0034

38. Lignani G, Raimondi A, Ferrea E, Rocchi A, Paonessa F, Cesca F, Orlando M, Tkatch T, Valtorta F, Cossette P, Baldelli P, Benfenati F (2013) Epileptogenic Q555X SYN1 mutant triggers imbalances in release dynamics and short-term plasticity. Hum Mol Genet 22 (11):2186-2199. doi:10.1093/hmg/ddt071

39. Verstegen AM, Tagliatti E, Lignani G, Marte A, Stolero T, Atias M, Corradi A, Valtorta F, Gitler D, Onofri F, Fassio A, Benfenati F (2014) Phosphorylation of synapsin I by cyclin-dependent kinase-5 sets the ratio between the resting and recycling pools of synaptic vesicles at hippocampal synapses. J Neurosci 34 (21):7266-7280. doi:10.1523/JNEUROSCI.3973-13.2014

40. Fassio A, Patry L, Congia S, Onofri F, Piton A, Gauthier J, Pozzi D, Messa M, Defranchi E, Fadda M, Corradi A, Baldelli P, Lapointe L, St-Onge J, Meloche C, Mottron L, Valtorta F, Khoa Nguyen D, Rouleau GA, Benfenati F, Cossette P (2011) SYN1 loss-of-function mutations in autism and partial epilepsy cause impaired synaptic function. Hum Mol Genet 20 (12):2297-2307. doi:10.1093/hmg/ddr122

41. Stevens CF (1993) Quantal release of neurotransmitter and long-term potentiation. Cell 72 Suppl:55-63

42. De Gois S, Schafer MK, Defamie N, Chen C, Ricci A, Weihe E, Varoqui H, Erickson JD (2005) Homeostatic scaling of vesicular glutamate and GABA transporter expression in rat neocortical circuits. J Neurosci 25 (31):7121-7133. doi:10.1523/JNEUROSCI.5221-04.2005

43. Herman MA, Ackermann F, Trimbuch T, Rosenmund C (2014) Vesicular glutamate transporter expression level affects synaptic vesicle release probability at hippocampal synapses in culture. J Neurosci 34 (35):11781-11791. doi:10.1523/JNEUROSCI.1444-14.2014

44. Muller M, Liu KS, Sigrist SJ, Davis GW (2012) RIM controls homeostatic plasticity through modulation of the readily-releasable vesicle pool. J Neurosci 32 (47):16574-16585. doi:10.1523/JNEUROSCI.0981-12.2012

45. Cesca F, Baldelli P, Valtorta F, Benfenati F (2010) The synapsins: key actors of synapse function and plasticity. Prog Neurobiol 91 (4):313-348. doi:10.1016/j.pneurobio.2010.04.006

46. Wu LG, Hamid E, Shin W, Chiang HC (2014) Exocytosis and endocytosis: modes, functions, and coupling mechanisms. Annu Rev Physiol 76:301-331. doi:10.1146/annurev-physiol-021113-170305

47. Zhao C, Dreosti E, Lagnado L (2011) Homeostatic synaptic plasticity through changes in presynaptic calcium influx. J Neurosci 31 (20):7492-7496. doi:10.1523/JNEUROSCI.6636-10.2011

48. Ooi L, Wood IC (2007) Chromatin crosstalk in development and disease: lessons from REST. Nat Rev Genet 8 (7):544-554. doi:10.1038/nrg2100

49. Roopra A, Dingledine R, Hsieh J (2012) Epigenetics and epilepsy. Epilepsia 53 Suppl 9:2-10. doi:10.1111/epi.12030

50. Hwang JY, Kaneko N, Noh KM, Pontarelli F, Zukin RS (2014) The gene silencing transcription factor REST represses miR-132 expression in hippocampal neurons destined to die. J Mol Biol 426 (20):3454-3466. doi:10.1016/j.jmb.2014.07.032

51. Zhao Y, Zhu M, Yu Y, Qiu L, Zhang Y, He L, Zhang J (2016) Brain REST/NRSF Is Not Only a Silent Repressor but Also an Active Protector. Mol Neurobiol. doi:10.1007/s12035-015-9658-4

52. Rodenas-Ruano A, Chavez AE, Cossio MJ, Castillo PE, Zukin RS (2012) REST-dependent epigenetic remodeling promotes the developmental switch in synaptic NMDA receptors. Nat Neurosci 15 (10):1382-1390. doi:10.1038/nn.3214

53. Garriga-Canut M, Schoenike B, Qazi R, Bergendahl K, Daley TJ, Pfender RM, Morrison JF, Ockuly J, Stafstrom C, Sutula T, Roopra A (2006) 2-Deoxy-D-glucose reduces epilepsy progression by NRSF-CtBP-dependent metabolic regulation of chromatin structure. Nat Neurosci 9 (11):1382-1387. doi:10.1038/nn1791

54. Hu XL, Cheng X, Cai L, Tan GH, Xu L, Feng XY, Lu TJ, Xiong H, Fei J, Xiong ZQ (2011) Conditional deletion of NRSF in forebrain neurons accelerates epileptogenesis in the kindling model. Cereb Cortex 21 (9):2158-2165. doi:10.1093/cercor/bhq284

55. Lu T, Aron L, Zullo J, Pan Y, Kim H, Chen Y, Yang TH, Kim HM, Drake D, Liu XS, Bennett DA, Colaiacovo MP, Yankner BA (2014) REST and stress resistance in ageing and Alzheimer's disease. Nature 507 (7493):448-454. doi:10.1038/nature13163

56. Nho K, Kim S, Risacher SL, Shen L, Corneveaux JJ, Swaminathan S, Lin H, Ramanan VK, Liu Y, Foroud TM, Inlow MH, Siniard AL, Reiman RA, Aisen PS, Petersen RC, Green RC, Jack CR, Jr., Weiner MW, Baldwin CT, Lunetta KL, Farrer LA, Study M, Furney SJ, Lovestone S, Simmons A, Mecocci P, Vellas B, Tsolaki M, Kloszewska I, Soininen H, AddNeuroMed C, McDonald BC, Farlow MR, Ghetti B, Indiana M, Aging S, Huentelman MJ, Saykin AJ, Alzheimer's Disease Neuroimaging I (2015) Protective variant for hippocampal atrophy identified by whole exome sequencing. Ann Neurol 77 (3):547-552. doi:10.1002/ana.24349

57. Yankner BA (2015) REST and Alzheimer disease. Ann Neurol 78 (3):499. doi:10.1002/ana.24420

Figure Legends

Figure 1. The frequency, but not the amplitude, of mEPSCs is scaled-down by REST increase induced by neuronal hyperactivity

A. Graphical representation of the experimental procedure. Mouse hippocampal primary cultures (16 div) were divided in 6 experimental groups: 1) control (ctrl, *white*), 2) treated with 4AP (100 μM) for 48 h (4AP, *grey*); 3,4), infected (10div) with either scramble shRNA (3; scr, *orange*) or REST shRNA (4; sh, *light blue*) and no further treated; 5,6) infected (10div) with either scramble shRNA (5; *scr-4AP, red*) or REST shRNA (6; *sh-4AP, blue*) and treated with 4AP for 48h. **B.** Representative mEPSCs traces recorded from indicated groups at 18div. **C.** Cumulative histograms of mEPSC inter-event intervals (*left*) and amplitude (*right*) under control condition (ctrl, *white,* n=40) and after treatment with 4AP for 48h (4AP, *grey,* n=33). The insets represent the mean (±SEM) of mEPSC frequency and amplitude (** $p<0.01$; *** $p<0.001$; Mann–Whitney's non-parametric U test). **D.** Mean ± SEM of mEPSC frequency (*left*) and amplitude (*right*) of scr (n=21), scr-4AP (n=19), sh (n=18) and sh-4AP (n=17) neurons. Two-way ANOVA followed by Sidak multi-comparison post-hoc test, of untreated *vs* 4AP treated neurons (*) and of scramble *vs* shRNA infected neurons (°). ** $p<0.01$, ***, °°° $p<0.001$.

Figure 2. REST induction by 4AP reduces the intensity of putative excitatory synaptic contacts.

A. Representative staining for β3-Tubulin (*green, left*), VGLUT1 (*red, middle*), and merge picture (*right*) with DAPI staining (*blue*) of hippocampal neurons that were either untreated (*top*) or treated for 48 h with 4AP (*bottom*). Scale bar, 15 μm. On the right, high magnification of a dendritic branch stained for β3-Tubulin (*green*) and VGLUT1 (*red*). Scale bar, 2 μm. **B.** Bars plot show the mean ± SEM values of fluorescence intensity of

VGLUT1-positive puncta (*left*) and number of VGLUT1-positive puncta per µm (*right*) in untreated (n=17 independent experiments, white) and 4AP-treated (n=6 independent experiments, *grey*) hippocampal neurons. **p<0.01; Mann–Whitney's U test. **C.** Mean ± SEM values of fluorescence intensity *(left)* and number of VGLUT1-positive puncta per µm *(right)* in *scr* (n=15), *scr-4AP* (n=15), *sh* (n=8) and *sh-4AP* (n=11) neurons. Two-way ANOVA followed by Sidak multi-comparison post-hoc test, of untreated *vs* 4AP treated neurons (*) and of scramble *vs* shRNA infected neurons (°). *** p<0.001, ° p<0.05.

Figure 3. REST exerts its homeostatic action through the modulation of SVs pools

A. Representative fluorescence images of neuronal processes co-infected with SypHy-GFP and with scr or shRNA upon various stimulation protocols. At rest, SypHy fluorescence is quenched by the intraluminal acidic pH of the SV. Upon electrical stimulation (2 sec@20 Hz), SVs fuse with the plasma membrane exposing the lumen to the neutral pH of the extracellular medium and causing an increase in SypHy fluorescence. The images show, from left to right, SypHy-positive puncta: 1) at rest*;* 2) at the peak of a response elicited by 40 APs at 20 Hz used to estimate the RRP size; 3) at the peak of a response elicited by 900 APs at 20 Hz used to estimate the recycling pool (RP)*;* and 4) after alkalinization with 50 mM NH_4Cl to estimate the total amount of SypHy-GFP expressed in the terminal. Scale bar, 10 µm. **B.** Average of SypHy fluorescence in scr- (*left*; n=11 experiments), and shRNA-(*right*; n=12 experiments) infected neurons stimulated with 40 APs at 20 Hz in the presence (*red and blue traces*) or absence (*orange and light blue traces*) of 100 µM 4AP. Data represent the time-course of the mean (±SEM) values of the change in ΔF values ($F-F_0$) normalized to the maximum fluorescence intensity reached under NH_4Cl perfusion (F_{max}). **C.** Bar histogram represents mean (±SEM) of the RRP size estimated as the peak $\Delta F/F_{max}$ evoked by the brief tetanic stimulation of

40 APs at 20 Hz. Two-way ANOVA followed by Sidak multi-comparison post-hoc test, of untreated *vs* 4AP treated neurons (*) and of scramble *vs* shRNA infected neurons (º). * p<0.05, ** p<0.01, °°° p<0.001. **D.** Ensemble average traces of SypHy fluorescence changes in response to stimulation with 900 APs at 20 Hz (*shaded area*) in the presence of bafilomycin (1 μM), in untreated and 4AP-treated neurons that had been infected with either scr *(left; n=8)* or shRNA *(right, n=8)*. Data represent the time-course of the mean (±SEM) of $\Delta F/F_{max}$ values. **E.** Bar histogram represents mean (±SEM) of the recycling pool (RP) size estimated at the $\Delta F/F_{max}$ plateau reached during by the long-lasting tetanic stimulation of 900 APs at 20 Hz in the presence of bafilomycin. Two-way ANOVA followed by Sidak multi-comparison post-hoc test, of untreated *vs* 4AP treated neurons (*) and of scramble *vs* shRNA infected neurons (º). ** p<0.01, °°° p<0.001.

Figure 4. Ultrastructural analysis of excitatory presynaptic site revealed a REST-dependent reduction of the density of docked SVs in response to hyperactivity.

A. Representative electron micrographs of neurons infected with either scr or shRNA, before and after treatment with 4AP. Scale bar, 200 nm. **B.** Mean (± SEM) of total SV density (*top)* and docked SV density *(bottom)*. n=90 synaptic terminals analysed from 3 independent preparations. Two-way ANOVA followed by Sidak multiple comparisons test between treatments (*) and groups (°).*** p<0.001; °°° p<0.001.

Figure 5. mRNA levels of presynaptic proteins are downregulated upon 4AP treatment in a REST-dependent manner.

A. RT-qPCR analysis of changes (means ± SEM) of REST (*upper panel*), AMPA1 (*center panel*) and VGLUT1 (*lower panel*) mRNA transcript levels in untreated neurons or in neurons treated with 4AP for 24 and 48h. All values are normalized to the scr level. Two-

way ANOVA followed by Sidak multiple comparisons test between treatments (*) and groups (°). * p<0,05, ** p<0.01, *** p<0.001, untreated *vs* 4AP-treated neurons; °°° p<0.001 scr *vs* sh-treated neurons. For each time point, n=16 from 8 independent neuronal preparations. **B.** Bar histograms of the means (± SEM) changes in SNAP 25 *(upper panel)*, Synapsin 1 *(center panel)* and Synaptotagmin 2 *(lower panel)* mRNA transcript levels in untreated and 4AP-treated (24 and 48 h) neurons that had been infected with either scr- and shRNA-infected neurons. For each time point, n=11 from 6 independent neuronal preparations. Two-way ANOVA followed by Sidak multiple comparisons test between treatments (*) and groups (°). *p<0.05, ** p<0.01; ° p<0.05.

Figure 1

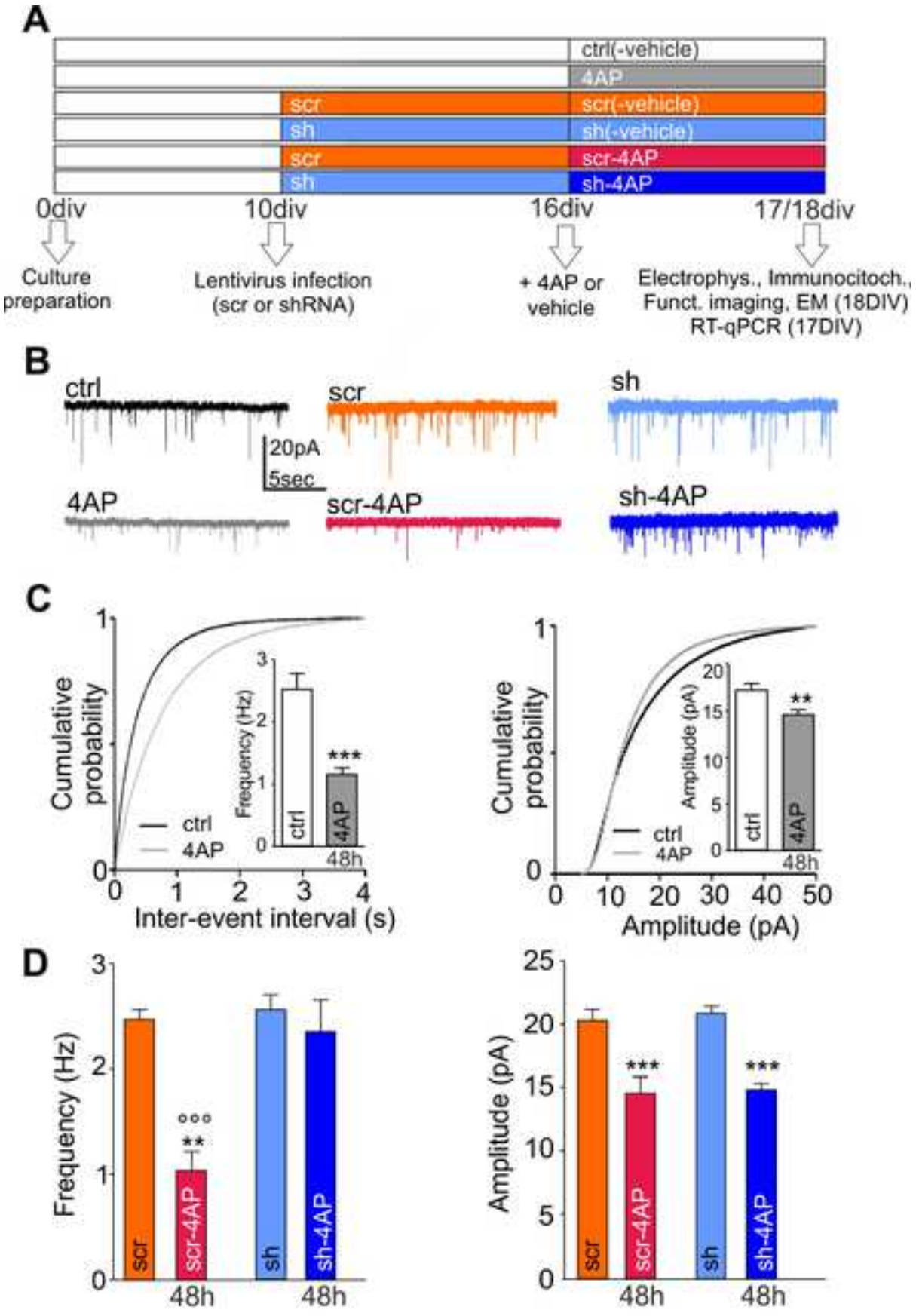

Figure 1

Figure 2

Click here to download Figure Figure 2.tif

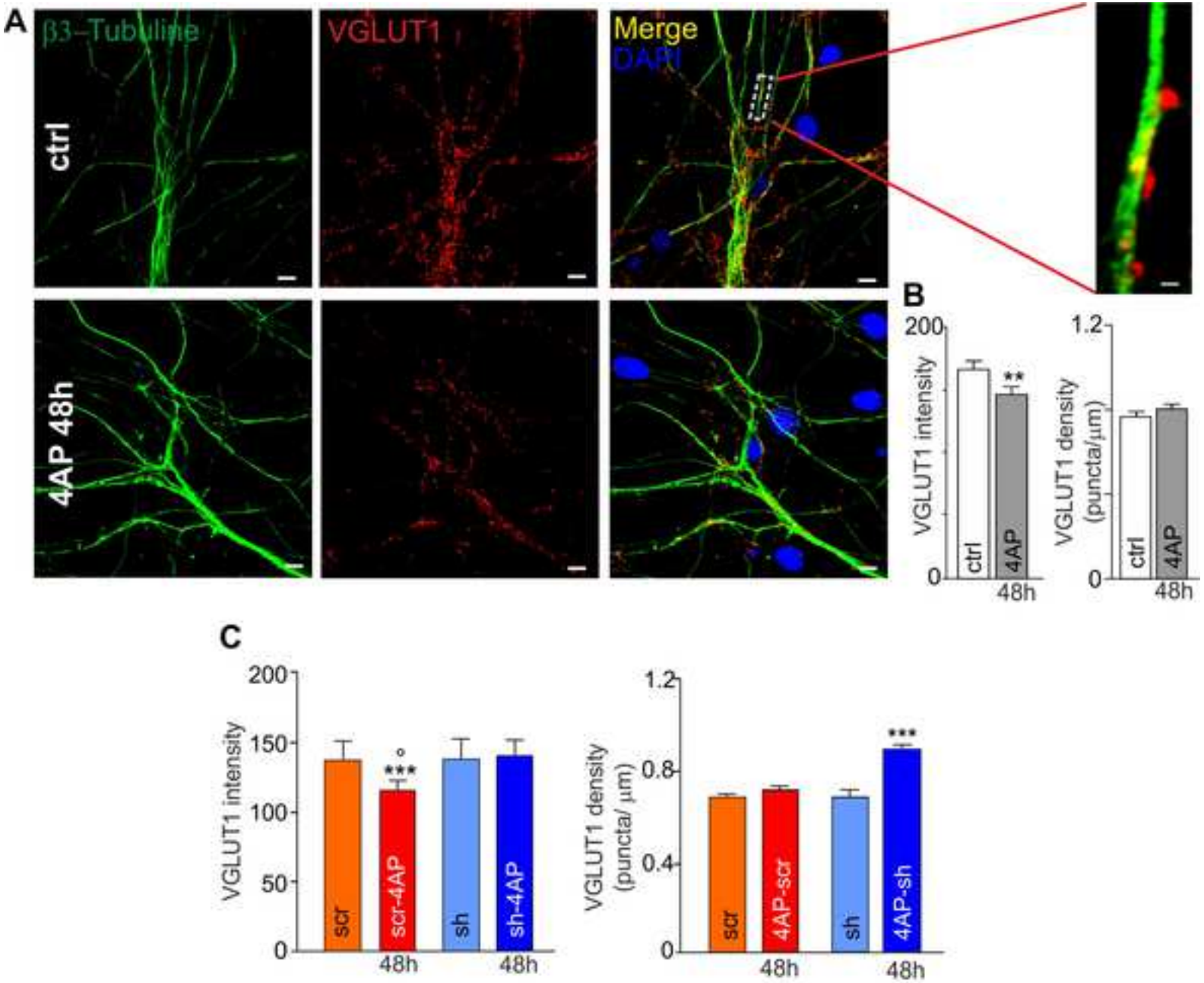

Figure 2

Figure 3

Click here to download Figure Figure 3.tif

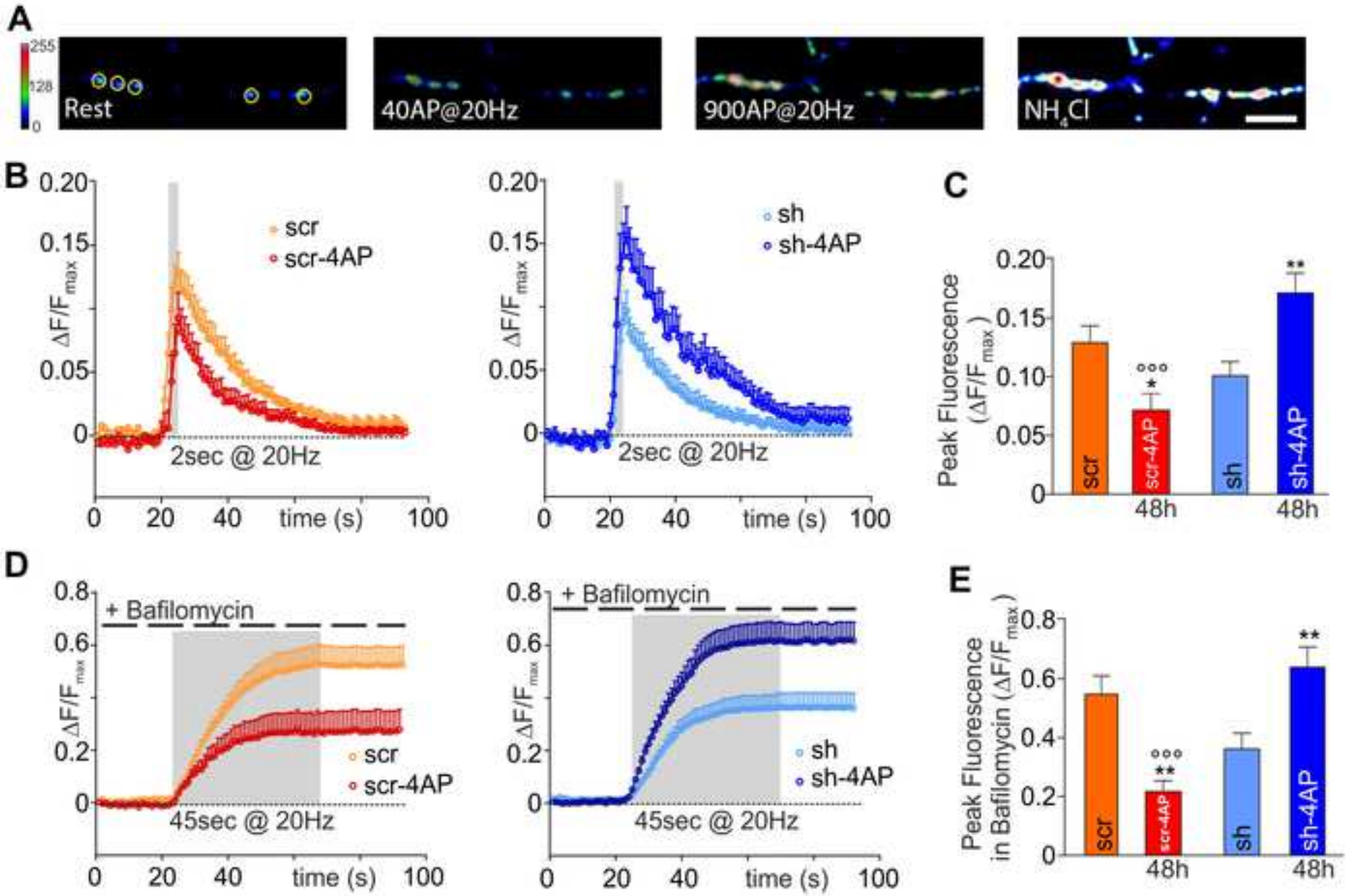

Figure 3

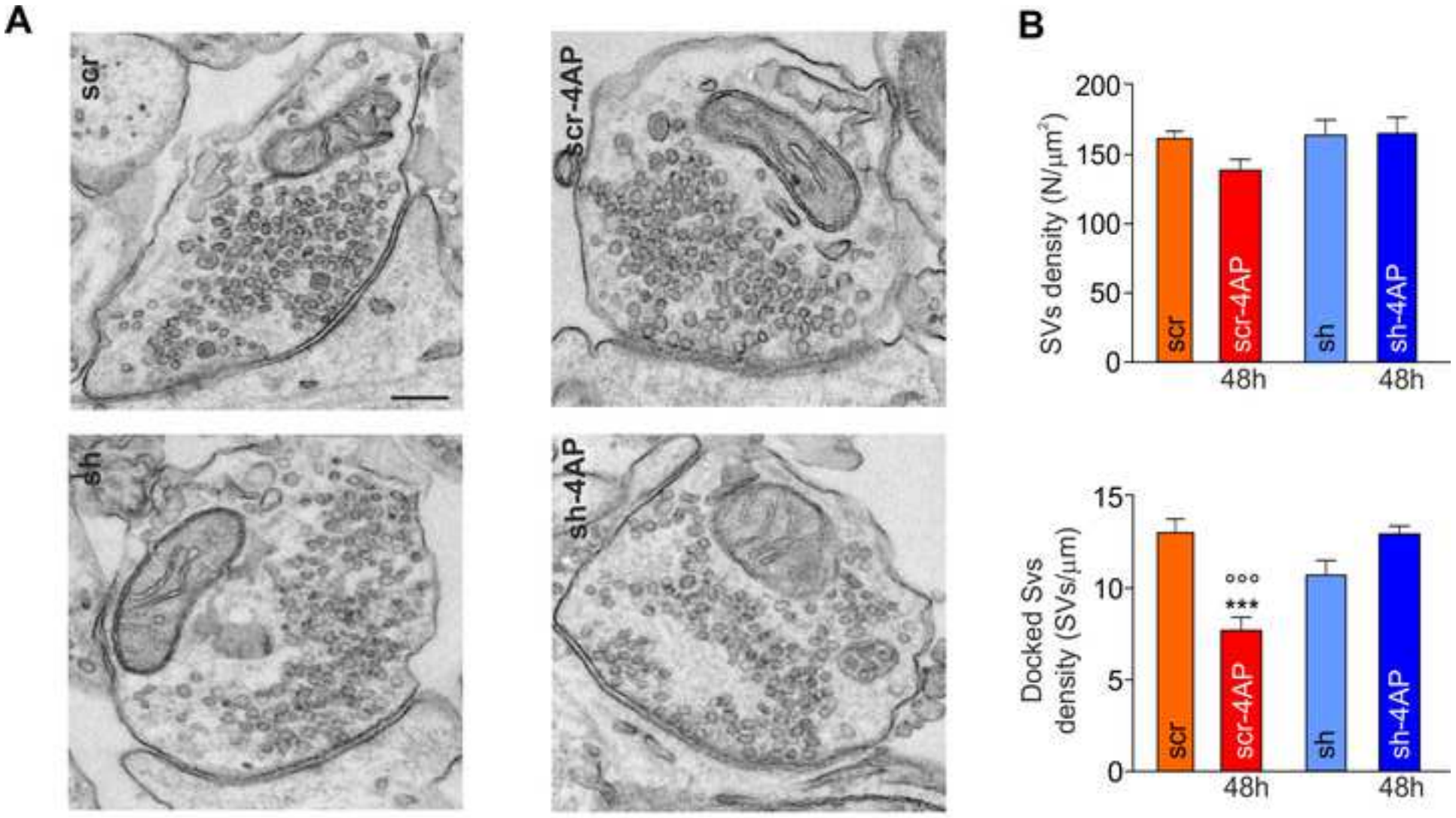

Figure 4

Figure 5

Click here to download Figure Figure 5.tif

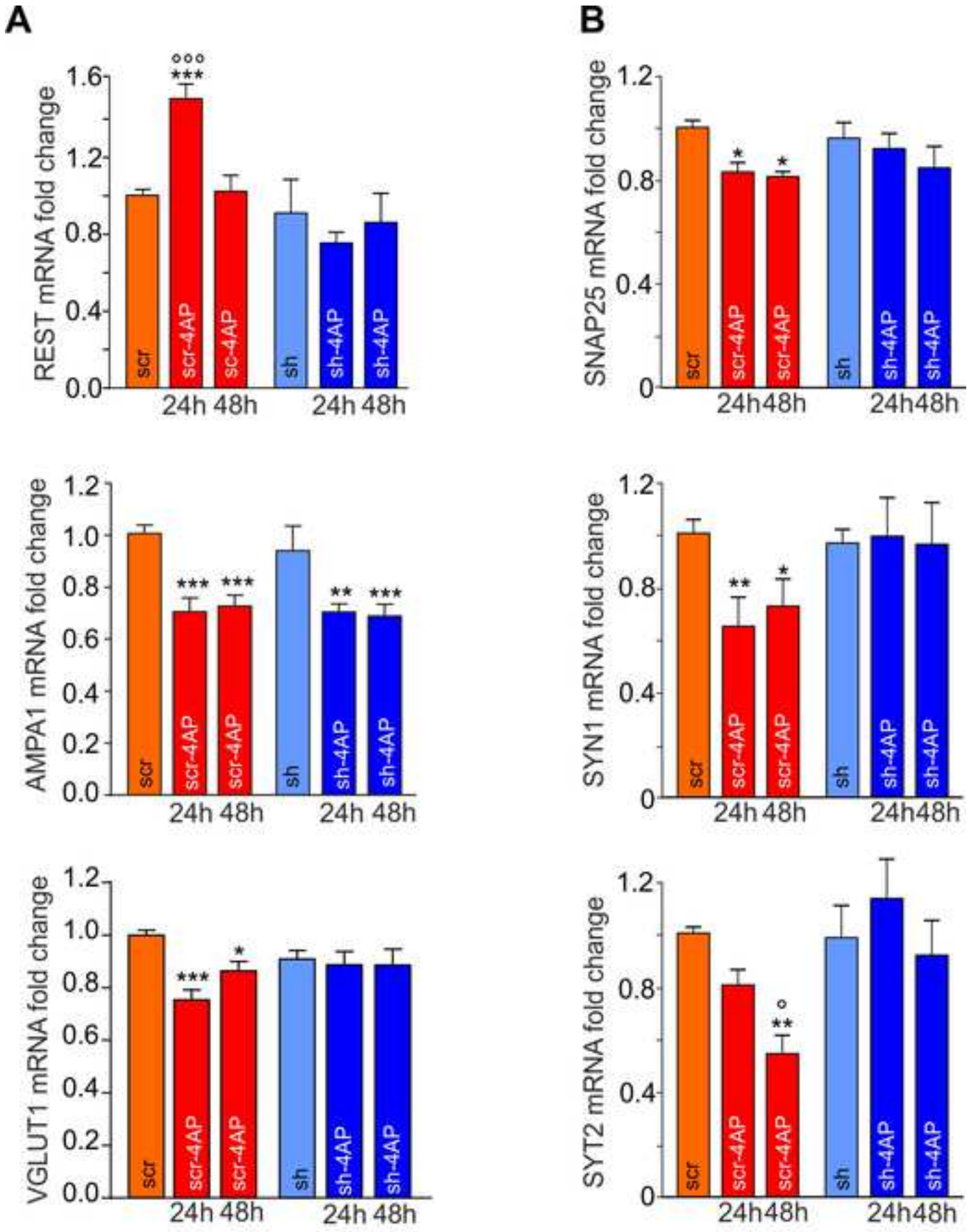

Figure 5